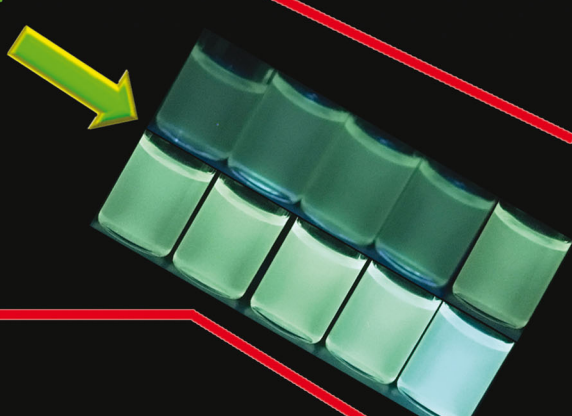
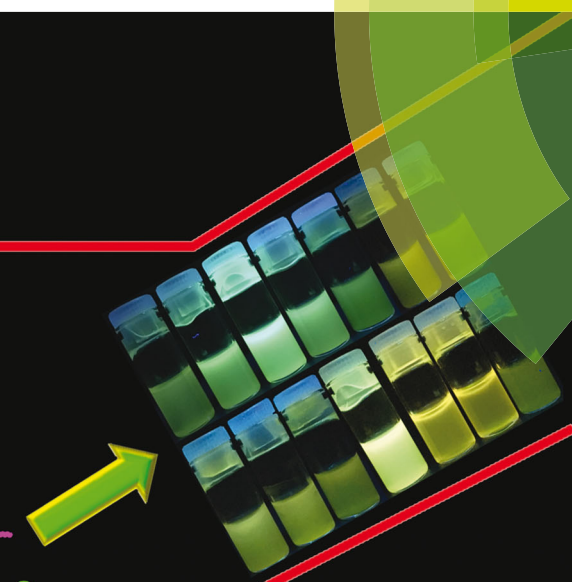
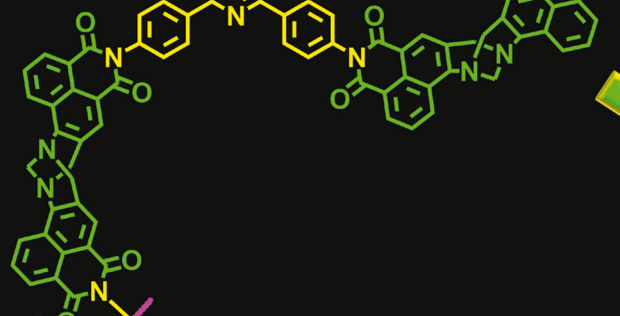
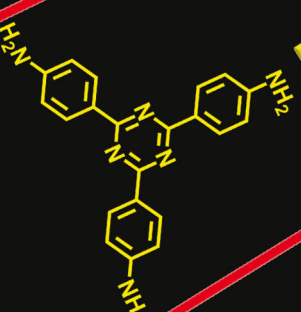
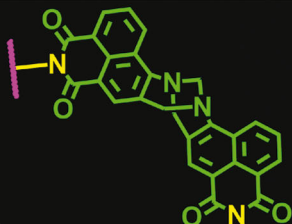
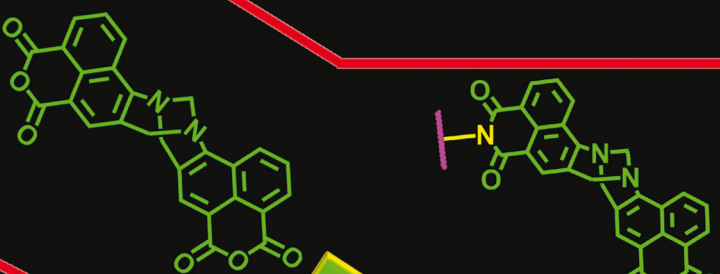


# ChemComm

Chemical Communications

rsc.li/chemcomm



ISSN 1359-7345



ROYAL SOCIETY  
OF CHEMISTRY

Celebrating  
IYPT 2019

## COMMUNICATION

Sankarasekaran Shanmugaraju,

Thorfinnur Gunnlaugsson *et al.*

"Turn-on" fluorescence sensing of volatile organic compounds using a 4-amino-1,8-naphthalimide Tröger's base functionalised triazine organic polymer



Cite this: *Chem. Commun.*, 2019, 55, 12140

Received 19th July 2019,  
Accepted 9th September 2019

DOI: 10.1039/c9cc05585a  
[rsc.li/chemcomm](http://rsc.li/chemcomm)

## "Turn-on" fluorescence sensing of volatile organic compounds using a 4-amino-1,8-naphthalimide Tröger's base functionalised triazine organic polymer†

Sankarasekaran Shanmugaraju, \*<sup>ab</sup> Deivasigamani Umadevi, <sup>c</sup>  
Luis M. González-Barcia, <sup>a</sup> Jason M. Delente, <sup>ad</sup> Kevin Byrne, <sup>c</sup>  
Wolfgang Schmitt, Graeme W. Watson<sup>c</sup> and Thorfinnur Gunnlaugsson \*<sup>ad</sup>

The 4-amino-1,8-naphthalimide Tröger's base functionalized triazine covalent organic polymer TB-TZ-COP was synthesised and employed as a "turn-on" fluorescent and a colorimetric sensor for the discriminative sensing of volatile organic compounds; the TB-TZ-COP displaying the largest fluorescent enhancement and high sensitivity for 1,4-dioxane, a harmful environmental pollutant classified as a Group 2B carcinogen.

Discovery of suitable chemosensors for the fast and selective sensing of hazardous substances and organic pollutants has attracted increasing attention in recent years to mitigate environmental pollution.<sup>1,2</sup> Among the various known pollutants, the volatile organic compounds (VOCs) have become a major source of environmental contaminants due to their mass use in manufacturing industries, as well as in scientific research laboratories.<sup>3</sup> The continuous exposure to VOCs is toxic to human health, causing a wide range of serious inflictions and chronic diseases like asthma, kidney failure, neurological damage, cystic fibrosis, and cancer.<sup>4,5</sup> Therefore, the design and the development of suitable chemical sensors for VOCs is highly desirable for the betterment of human health and to get rid of environmental pollution.<sup>6</sup> Several sophisticated instrumental techniques are currently available for VOCs detection and analysis, including gas-chromatography, high-performance liquid chromatography, ion chromatography, and mass spectrometry.<sup>3,4,6,7</sup> Despite the high selectivity, the real-time use of these traditional techniques

is limited due to their expensive apparatuses, lack of portability, time-consuming detection process, and complicated instrument standardization.<sup>6,7</sup> Recently, fluorescence quenching/enhancement-based sensing has become an effective and alternative detection method to the above, owing to its simplicity, high sensitivity, easy visualization and short response time;<sup>1,2,8,9</sup> where the initial emission intensity of the fluorophore is perturbed, in one way or the other, by the presence of analytes.<sup>10</sup> A wide variety of fluorescent sensors have been developed and used for the detection of VOCs through fluorescence quenching based mechanism; however, background interference has been known to limits their practical use.<sup>11</sup> Furthermore, their real-life application has also been restricted due to low sensitivity, non-reusability and lack of specificity among VOCs.<sup>12</sup> Hence, there currently exists a need for developing alternative analytical/sensing methods for VOCs. In general, the use of 'turn-on' (also known as 'switch-on') fluorescence sensing is particularly appealing because the sensing event can be easily detected, sometimes, even by the naked eye.<sup>13</sup> However, unlike 'turn-off' sensing, which can simply operate *via* static or dynamic quenching mechanisms, the design of *turn-on* fluorescence sensing, is more challenging.<sup>14</sup> We thus considered if the use of solvatochromic fluorescent sensing, might be a simple and an effective alternative and an effective approach for the discriminative sensing of VOCs.<sup>15,16</sup> With this in mind, we set out to develop an efficient fluorescent sensor suitable for selective and discriminative sensing of structurally related-VOCs, based on amino-1,8-naphthalimide Tröger's bases (TBNaps).

Over the past few years, we are interested in developing novel luminescent structures and materials of 3- and 4-amino-TBNaps motifs for their application in supramolecular material and medicinal chemistry.<sup>17</sup> TBNaps are fascinating chiral cleft-shaped supramolecular scaffolds (with *ca.* 90° angle between the two Nap structures) that are strongly colored and fluorescent due to their internal charge-transfer (ICT) excited state transition; which are solvent polarity dependent.<sup>2,17</sup> Furthermore, TBNaps display significant Stokes shifts in different solvents and thus they can be used as a potential luminescent sensor for the

<sup>a</sup> School of Chemistry and Trinity Biomedical Sciences Institute (TBSI), Trinity College Dublin, The University of Dublin, Dublin 2, Ireland.

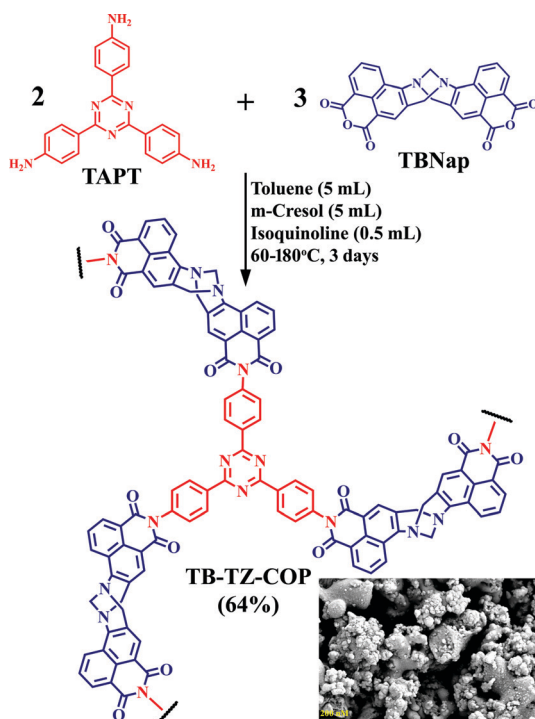
E-mail: gunnlaut@tcd.ie

<sup>b</sup> Chemistry, Indian Institute of Technology Palakkad (IITPKD), Palakkad 678557, Kerala, India. E-mail: shamugam@iitpkd.ac.in

<sup>c</sup> School of Chemistry and Centre for Research on Adaptive Nanostructures and Nanodevices (CRANN), Trinity College Dublin, The University of Dublin, Dublin 2, Ireland

<sup>d</sup> Advanced Materials and BioEngineering Research Center (AMBER), Trinity College Dublin, Dublin 2, Ireland

† Electronic supplementary information (ESI) available: Experimental details, synthesis and characterisation details (FTIR, TGA, powder diffraction and SEM) fluorescence studies and computational details. See DOI: 10.1039/c9cc05585a



Scheme 1 Synthesis of polyimide TB-TZ-COP (inset: FESEM image of as-synthesized polymer).

discriminative sensing of structurally similar VOCs of varied polarity. Here we report the synthesis and fluorescence sensing properties of a new TBNap functionalized triazine covalent organic polymer, TB-TZ-COP, Scheme 1. We foresaw that the polyimide part of TB-TZ-COP would structurally facilitate the solvent polarity dependent emission properties, and thus TB-TZ-COP could act as a potential fluorescence sensor for the discriminative sensing of volatile organic pollutants.<sup>2,9</sup>

The polyimide TB-TZ-COP was synthesized using a one-step metal-free polycondensation reaction, Scheme 1, between triazine-based triamine (TAPT, 2.0 eq.) and the 4-amino-1,8-naphthalic anhydride derived Tröger's base (TBNap, 3.0 eq.) in a mixture of toluene and *m*-cresol as a reaction medium and isoquinoline as a catalyst under a stepwise increase of the reaction temperature (for details see ESI†).<sup>18,19</sup> The TB-TZ-COP polymer was isolated as a bright yellow solid and was found to be insoluble in common organic solvents. The successful formation of TB-TZ-COP was fully characterized at the molecular level by using CP/MAS <sup>13</sup>C-NMR and FT-IR spectroscopy. The solid-state <sup>13</sup>C-NMR spectrum of TB-TZ-COP showed the expected characteristic carbonyl carbon resonances at 164 ppm, which is slightly down-field shifted (~2 ppm) compared to the TBNap monomer due to the imide ring formation (ESI†).<sup>19,20</sup> The signal corresponding to the triazine unit was clearly observed at 171 ppm, while the two CH<sub>2</sub> carbon resonances of Tröger's base linkage were located at 67 and 57 ppm.<sup>20</sup> The chemical shifts corresponding to the other aromatic carbons were observed as a hampered overlapping signal in the range of 118 to 150 ppm (ESI†). In the FT-IR spectrum, the appearance of a new broad band at 1353 cm<sup>-1</sup> corresponding to the stretching vibration of C-N-C linkage of the

imide ring and the complete disappearance of NH<sub>2</sub> stretching vibrations around 3314 cm<sup>-1</sup> of TAPT monomer confirms the successful formation of polyimide network in the isolated material (ESI†).<sup>21</sup> The characteristics carbonyl symmetric and asymmetric stretching vibrations of six-membered imide ring were observed at 1707 cm<sup>-1</sup> and 1666 cm<sup>-1</sup>, respectively. The FT-IR spectra also showed several intense bands at 1240 cm<sup>-1</sup> and 1503 cm<sup>-1</sup> accounting for C-N and N-C-N stretching, respectively which confirms the successful incorporation of Tröger's base and triazine functional groups into the isolated material (ESI†). The elemental analysis of TB-TZ-COP indicated that the calculated elemental composition is consistent with the experimentally measured values. The thermogravimetric analysis (TGA) under N<sub>2</sub> atmosphere showed an initial weight loss of ~4% at low temperature due to the loss of trapped solvent molecules and the desolvated TB-TZ-COP was stable up to 410 °C, indicating its high thermal stability (ESI†). The powder X-ray diffraction (PXRD) measurement shows that TB-TZ-COP was amorphous in nature (ESI†). The morphology of TB-TZ-COP, as observed by FESEM, is composed of particles with a rough surface and in a disorganized pattern (Scheme 1 and ESI†). The surface area and porosity of TB-TZ-COP were verified by N<sub>2</sub> adsorption isotherm. The N<sub>2</sub> uptake measurement at 77 K of activated TB-TZ-COP displayed steep and reversible adsorption of 139 cm<sup>3</sup> g<sup>-1</sup> at 1 bar (ESI†). The Brunauer–Emmett–Teller (BET) surface was calculated to be 198 m<sup>2</sup> g<sup>-1</sup>. The DFT pore size distribution confirms the presence of microporosity. Notably, the uptake capacity of TB-TZ-COP for CO<sub>2</sub> was moderate while the uptake capacity for H<sub>2</sub> was almost negligible (ESI†). The presence of high surface area and micropores suggests that TB-TZ-COP can, in addition to the surface interactions, efficiently adsorb the analytes inside the voids space and thus it can show superior sensing capability.<sup>2</sup>

Having successfully synthesized and characterized TB-TZ-COP, we next looked into the fluorescence sensing characteristics of TB-TZ-COP towards VOCs. These experiments were performed by dispersing TB-TZ-COP in various common organic solvents with varying polarities, such as toluene, CH<sub>2</sub>Cl<sub>2</sub>, THF, acetone, CH<sub>3</sub>OH, CH<sub>3</sub>CH<sub>2</sub>OH, CH<sub>3</sub>CN, diethyl ether, glycol, 1,4-dioxane, DMF, DMSO and then measured the fluorescence emission intensity of TB-TZ-COP in these solvents. As expected, the suspension of TB-TZ-COP displayed different fluorescent emission characteristics in these solvents and thus discriminative sensing ability for the rapid detection of VOCs (Fig. 1). Notably, the suspension of TB-TZ-COP in 1,4-dioxane displayed a dramatic enhancement in the fluorescence intensity in comparison to other organic solvents tested for. Furthermore, the discriminative sensing ability of TB-TZ-COP was found to be highly sensitive and reversible.

The emission intensity in H<sub>2</sub>O was used as a reference to determine the relative number-fold emission enhancement of TB-TZ-COP in different organic solvents. The fluorescent study results implied that TB-TZ-COP was capable of discriminatively sense VOCs through a change in the TBNap fluorescence intensity, either *via* luminescent quenching or through luminescent enhancement (Fig. 1A). As alluded to above, then among different VOCs, the largest emission enhancement of 44% was observed at 502 nm for 1,4-dioxane, while THF, showed a moderate fluorescence

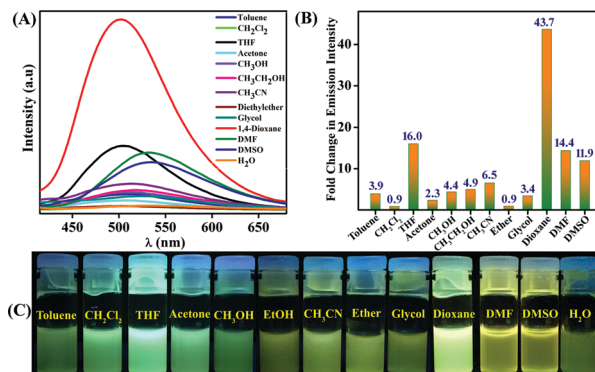


Fig. 1 (A) The emission spectra ( $\lambda_{\text{ex}} = 360 \text{ nm}$ ) of **TB-TZ-COP** in different solvents and (B) corresponding fold change in emission intensity with respect to its emission in  $\text{H}_2\text{O}$ . (C) Photograph of **TB-TZ-COP** dispersed in different solvents taken under UV light illumination ( $\lambda_{\text{ex}} = 365 \text{ nm}$ ).

enhancement ( $\sim 16\%$ ) upon exciting at 360 nm. In high polar solvents such as DMF and DMSO, **TB-TZ-COP** displayed an average emission enhancement, which was significantly red-shifted to around 534 nm with a large Stokes shift; this shift is accompanied by **TBNap** spectral broadening. This can be accounted for because the excited state of the **TBNap** fluorophore is more stabilized in highly polar solvents than the ground state due to increasing the non-radiative transition of excited molecules.<sup>16</sup> Notably, the suspension of **TB-TZ-COP** in other organic solvents displayed almost no to weak fluorescence emission intensity. As depicted in Fig. 1B, the descending order of relative fold-change in emission enhancement of **TB-TZ-COP** are as following: 1,4-dioxane > THF > DMF > DMSO > CH<sub>3</sub>CN > CH<sub>3</sub>CH<sub>2</sub>OH > CH<sub>3</sub>OH > toluene > glycol > acetone > CH<sub>2</sub>Cl<sub>2</sub>  $\approx$  diethyl ether. This results clearly demonstrate the discriminative sensing ability of **TB-TZ-COP** towards the closely related VOCs. Gratifyingly, this discriminative fluorescence sensing was also being clearly visible to the naked eye as it appears from Fig. 1C.

We further performed Density Functional Theory (DFT) calculations using Gaussian 09<sup>22</sup> on our system to elucidate the reasons for the observed discriminative fluorescence sensing. One monomer unit of **TB-TZ-COP** as a representative fragment was considered for optimization. We also modelled all the VOCs considered in this study. Geometry optimization was done using DFT by employing the hybrid M062X functional and 6-311G(d,p) basis set.<sup>23</sup> The highest occupied molecular orbital (HOMO) and the lowest unoccupied molecular orbital (LUMO) energies of the **TB-TZ-COP** and the VOCs were calculated. It has been suggested that the fluorescent enhancement may be due to the energy transfer from the VOCs to **TB-TZ-COP**; this classically will only happen when the LUMO of the analyte is higher in energy than the corresponding LUMO of the sensor.<sup>20</sup> Gratifyingly, the LUMO energies of all the analytes tested for were comparatively higher (see ESI,† Table S1) than that determined computationally for **TB-TZ-COP** which would facilitate the energy transfer that gives rise to the fluorescence emission. While this would be in support of the observed emission enhancement (of 44%) for 1,4-dioxane, which has the highest LUMO energy value for the solvents studied, it would not account entirely for the observed order of

enhancement seen for the other VOCs. Hence, the energy transfer phenomenon might not be the sole mechanism for the observed emission enhancements, and in fact, alternative and weak interaction might also be operating between **TB-TZ-COP** and the VOCs, which would further contribute to the observed luminescence enhancement. It has been shown that 1,4-dioxane exhibit significant intermolecular interactions with the solute, especially with aromatic molecules.<sup>24</sup> Because of this, we set out to investigate the fluorescent sensing of 1,4-dioxane more thoroughly using **TB-TZ-COP**.

Despite its hazardous nature, 1,4-dioxane is still used as a solvent in a variety of practical application, and the solvent is considered as an environmental pollutant and classified as group 2B carcinogens by US EPA. It is also used as a stabilizer for the organochloride transport and as a precursor in various manufacturing industries.<sup>25</sup> In general, 1,4-dioxane is synthesized *via* the condensation reaction of ethylene glycol (Fig. 2A).<sup>26</sup> Hence, having a sensor that can distinguish between glycol and 1,4-dioxane is practically useful. The fluorescence emission intensity of polymer **TB-TZ-COP** in glycol, 1,4-dioxane, and their mixture were thus assessed. As shown in Fig. 2C, the emission intensity of **TB-TZ-COP** in glycol increased linearly with an increasing percentage volume ratio of 1,4-dioxane. This enhancement was also accompanied by a significant blue-shift of  $\sim 22 \text{ nm}$  in the fluorescence emission, assigned to the decrease in the polarity of the resulting solvent mixture. Furthermore, the effect was also clearly visible to the naked eye as is evident from Fig. 2B. Further analysis demonstrated fast emission response times, and a linear relationship between the observed emission enhancement and the concentrations of 1,4-dioxane in glycol; both demonstrating that **TB-TZ-COP** could be employed for the quantitative determination of specific VOCs mixtures (see ESI†). In fact, quantitative analysis of the emission enhancement profile

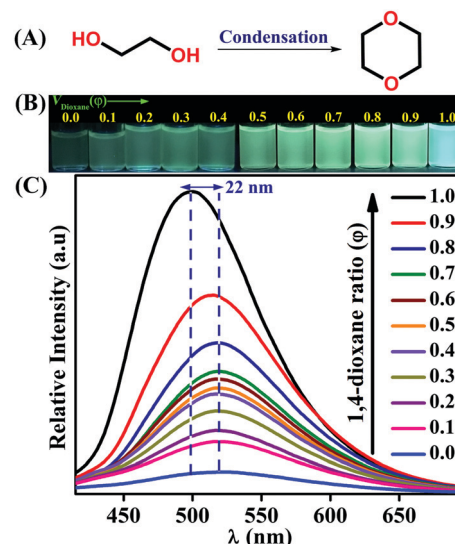
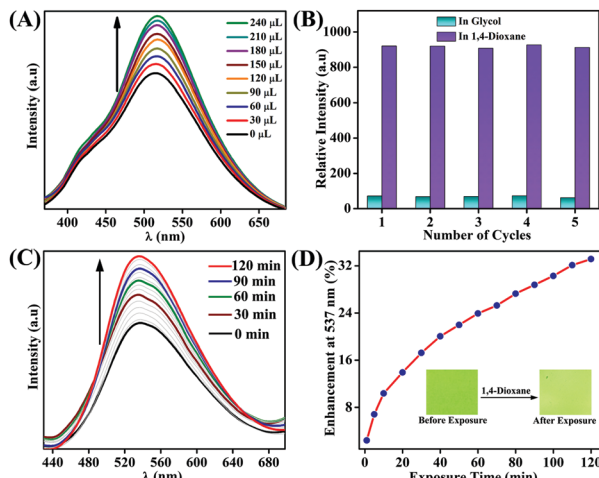


Fig. 2 (A) The reaction scheme for the condensation of glycol to 1,4-dioxane. (C) Emission spectra of **TB-TZ-COP** in glycol/1,4-dioxane mixture with different volume ratio of 1,4-dioxane and (B) corresponding photographs taken under UV light illumination ( $\lambda_{\text{ex}} = 365 \text{ nm}$ ).



**Fig. 3** (A) Change in emission intensity of **TB-TZ-COP** upon addition of dioxane ( $\mu\text{L}$ ) in glycol. (B) Recycling test in glycol and in dioxane. (C) Emission spectra of thin film of **TB-TZ-COP** upon exposure to the dioxane vapours and (D) its corresponding enhancement efficiency plot (inset: photograph of thin film of **TB-TZ-COP** before and after exposure to dioxane vapours).

did demonstrate that **TB-TZ-COP** could detect 1,4-dioxane in glycol at as low levels as 22.2 ppm (Fig. 3A and ESI†).<sup>11</sup>

To meet the practical application of the **TB-TZ-COP** polymer as a reversible fluorescence sensor, we next verified the reproducibility of the sensing process of **TB-TZ-COP** towards 1,4-dioxane. The emission intensity of **TB-TZ-COP** in both glycol and 1,4-dioxane was first recorded, and after each measurement, the polymer was isolated by centrifugation and subsequently reused in the next emission study (cycle). As shown in Fig. 3B, the emission intensity of **TB-TZ-COP** in glycol (cyan bar) and 1,4-dioxane (violet bar), was retained even after five cycles of repetitions. This study demonstrates the excellent reproducibility, the recyclability sensing and the high photostability of **TB-TZ-COP** over several sensing cycles. To further explore the vapor phase sensing propensity of **TB-TZ-COP**, the emission intensity of a freshly made thin film of **TB-TZ-COP** exposed to the saturated vapours of 1,4-dioxane was monitored as a function of exposure time. As can be seen in Fig. 3C, the initial emission intensity of **TB-TZ-COP** at 537 nm increased dramatically upon exposing the film to the saturated vapours of 1,4-dioxane at room temperature, indicating the strong binding interactions between analytes and polymer. For instance, the emission was enhanced by 17% after just 30 minutes of exposure time; reaching 33% within 120 minutes, as demonstrated in Fig. 3D. Furthermore, a noticeable visual colour change was observed upon exposing the film to 1,4-dioxane vapours, as presented as an inset in Fig. 3D, demonstrating the potential application of **TB-TZ-COP** as a naked eye sensor for both solution and vapor phase detection of VOCs.

In summary, we have synthesized a new **TBNap** functionalized triazine covalent organic polymer, **TB-TZ-COP**, and demonstrated its application in the discriminative fluorescence sensing of VOCs. Notably, the ability of **TB-TZ-COP** to distinguish between structurally and chemically close related VOCs, such as glycol and 1,4-dioxane, was demonstrated. Such a system is highly attractive, the sensing being achieved in both solution and in the vapor phase using thin films using either colorimetric or fluorescent

sensing. We are currently exploring the properties of such sensors in greater detail.

We thank the Irish Research Council for postdoctoral fellowships (GOIPD/2013/442 to SS and GOIPD/2015/290 to DU) and Science Foundation Ireland (SFI PI Award 13/IA/1865 to TG). We also thank Dr M. Ruether for carrying out NMR analysis of the monomer and polymer developed herein. All computational calculations were performed using the Lonsdale supercomputers at Trinity Centre for High-Performance Computing (TCHPC).

## Conflicts of interest

There are no conflicts to declare.

## Notes and references

- 1 D. Wu, A. C. Sedgwick, T. Gunnlaugsson, E. U. Akkaya, J. Yoon and T. D. James, *Chem. Soc. Rev.*, 2017, **46**, 7105–7123.
- 2 S. Shanmugaraju, C. Dabade, K. Byrne, A. J. Savyasachi, D. Umadevi, W. Schmitt, J. A. Kitchen and T. Gunnlaugsson, *Chem. Sci.*, 2017, **8**, 1535–1546.
- 3 R. Atkinson and J. Arey, *Chem. Rev.*, 2003, **103**, 4605–4638.
- 4 K. Vellingiri, P. Kumar and K.-H. Kim, *Nano Res.*, 2016, **9**, 3181–3208.
- 5 L. Mølhave, B. Bach and O. F. Pedersen, *Environ. Int.*, 1986, **12**, 167–175.
- 6 T. Kida, K. Suematsu, K. Hara, K. Kanie and A. Muramatsu, *ACS Appl. Mater. Interfaces*, 2016, **8**, 35485–35495.
- 7 D. S. Moore, *Rev. Sci. Instrum.*, 2004, **75**, 2499–2512.
- 8 Y. Cui, Y. Yue, G. Qian and B. Chen, *Chem. Rev.*, 2012, **112**, 1126–1162.
- 9 S. Shanmugaraju, S. A. Joshi and P. S. Mukherjee, *J. Mater. Chem.*, 2011, **21**, 9130–9138; S. Shanmugaraju and P. S. Mukherjee, *Chem. Commun.*, 2015, **51**, 16014–16032.
- 10 B. McLaughlin, E. M. Surrender, G. D. Wright, B. Daly and A. P. de Silva, *Chem. Commun.*, 2018, **54**, 1319–1322; A. J. Savyasachi, D. F. Caffrey, K. Byrne, G. Tobin, B. D'Agostino, W. Schmitt and T. Gunnlaugsson, *Front. Chem. Eng.*, 2019, **13**, 171–184.
- 11 D. Ma, B. Li, Z. Cui, K. Liu, C. Chen, G. Li, J. Hua, B. Ma, Z. Shi and S. Feng, *ACS Appl. Mater. Interfaces*, 2016, **8**, 24097–24103; J. Zhou, H. Li, H. Zhang, H. Li, W. Shi and P. Cheng, *Adv. Mater.*, 2015, **27**, 7072–7077.
- 12 R. Goswami, S. C. Mandal, B. Pathak and S. Neogi, *ACS Appl. Mater. Interfaces*, 2019, **11**, 9042–9053.
- 13 S. Erbas-Cakmak, S. Kolemen, A. C. Sedgwick, T. Gunnlaugsson, T. D. James, J. Yoon and E. U. Akkaya, *Chem. Soc. Rev.*, 2018, **47**, 2228–2248.
- 14 Y. Tang, D. Lee, J. Wang, G. Li, J. Yu, W. Lin and J. Yoon, *Chem. Soc. Rev.*, 2015, **44**, 5003–5015; P. Mani, A. A. Ojha, V. S. Reddy and S. Mandal, *Inorg. Chem.*, 2017, **56**, 6772–6775; L. Guao and D. Cao, *J. Mater. Chem. C*, 2015, **3**, 8490–8494.
- 15 L. Dai, D. Wu, Q. Qiao, W. Yin, J. Yin and Z. Xu, *Chem. Commun.*, 2016, **52**, 2095–2098; C. J. Chang, T. Gunnlaugsson and T. D. James, *Chem. Soc. Rev.*, 2015, **44**, 4176–4178.
- 16 R. M. Duke, E. B. Veale, F. M. Pfeffer, P. E. Kruger and T. Gunnlaugsson, *Chem. Soc. Rev.*, 2010, **39**, 3936–3953.
- 17 E. B. Veale, D. O. Frimannsson, M. Lawler and T. Gunnlaugsson, *Org. Lett.*, 2009, **11**, 4040–4043; E. B. Veale and T. Gunnlaugsson, *J. Org. Chem.*, 2010, **75**, 5513–5525.
- 18 Y. Luo, B. Li, L. Liang and B. Tan, *Chem. Commun.*, 2011, **47**, 7704–7706.
- 19 Q. Fang, Z. Zhuang, S. Gu, R. B. Kaspar, J. Zheng, J. Wang, S. Qiu and Y. Yan, *Nat. Commun.*, 2014, **5**, 4503.
- 20 Y. Liao, J. Weber and C. F. J. Faul, *Macromolecules*, 2015, **48**, 2064–2073; J. Dong, A. K. Tummanapelli, X. Li, S. Ying, H. Hirao and D. Zhao, *Chem. Mater.*, 2016, **28**, 7889–7897.
- 21 S. Shanmugaraju, D. Umadevi, A. J. Savyasachi, K. Byrne, M. Ruether, W. Schmitt, G. W. Watson and T. Gunnlaugsson, *J. Mater. Chem. A*, 2017, **5**, 25014–25024.
- 22 M. J. Frisch, *et al.*, *GAUSSIAN 09*, Gaussian Inc., Wallingford, CT, 2009.
- 23 Y. Zhao and D. Truhlar, *Theor. Chem. Acc.*, 2008, **120**, 215–241.
- 24 A. K. Nain, N. Chaudhury, Ankita, J. Gupta and P. Chandra, *J. Chem. Thermodyn.*, 2017, **108**, 145–161.
- 25 A. Abe, *Sci. Total Environ.*, 1999, **227**, 41–47.
- 26 A. J. Heuvelsland, *Method for Producing 1,4-Dioxane*, US 4764626, 1988.